The International Society of Precision Agriculture presents the

15th International Conference on
Precision Agriculture
26–29 JUNE 2022
Minneapolis Marriott City Center | Minneapolis, Minnesota USA

Increasing the Accuracy of UAV-Based Remote Sensing Data for Strawberry Nitrogen and Water Stress Detection

S. Bhandari[1], A. Raheja[2], and Mohammad Chaichi[3]

[1]Department of Aerospace Engineering; [2]Department of Computer Science; [3]Department of Plant Sciences;
California State Polytechnic University, Pomona, CA

**A paper from the Proceedings of the
15th International Conference on Precision Agriculture
June 26-29, 2022
Minneapolis, Minnesota, United States**

Abstract.

This paper presents the methods to increase the accuracy of unmanned aerial vehicles (UAV)-based remote sensing data for the determination of plant nitrogen and water stresses with increased accuracy. To increase the accuracy of remote sensing data, various methods were investigated. These include use of portable Ground Control Points and high performance GPS. Remote sensing data was collected from UAVs equipped with hyperspectral and multispectral sensors. To determine the effectiveness of the above methods, vegetation indices such as normalized difference vegetation index (NDVI), Green NDVI (GNDVI), and Water Band Index (WBI) calculated using the remote sensing data were compared with the data obtained from proximal sensors that include Handheld Spectroradiometer and Chlorophyll Meter. Correlations between different vegetation indices, chlorophyll meter data, and spectroradiometer data are shown for strawberry plants.

Keywords.
Ground control points, NDVI, WBI, LCI, Correlations

Introduction

As the demand for agricultural products is significantly increasing to keep up with the growing
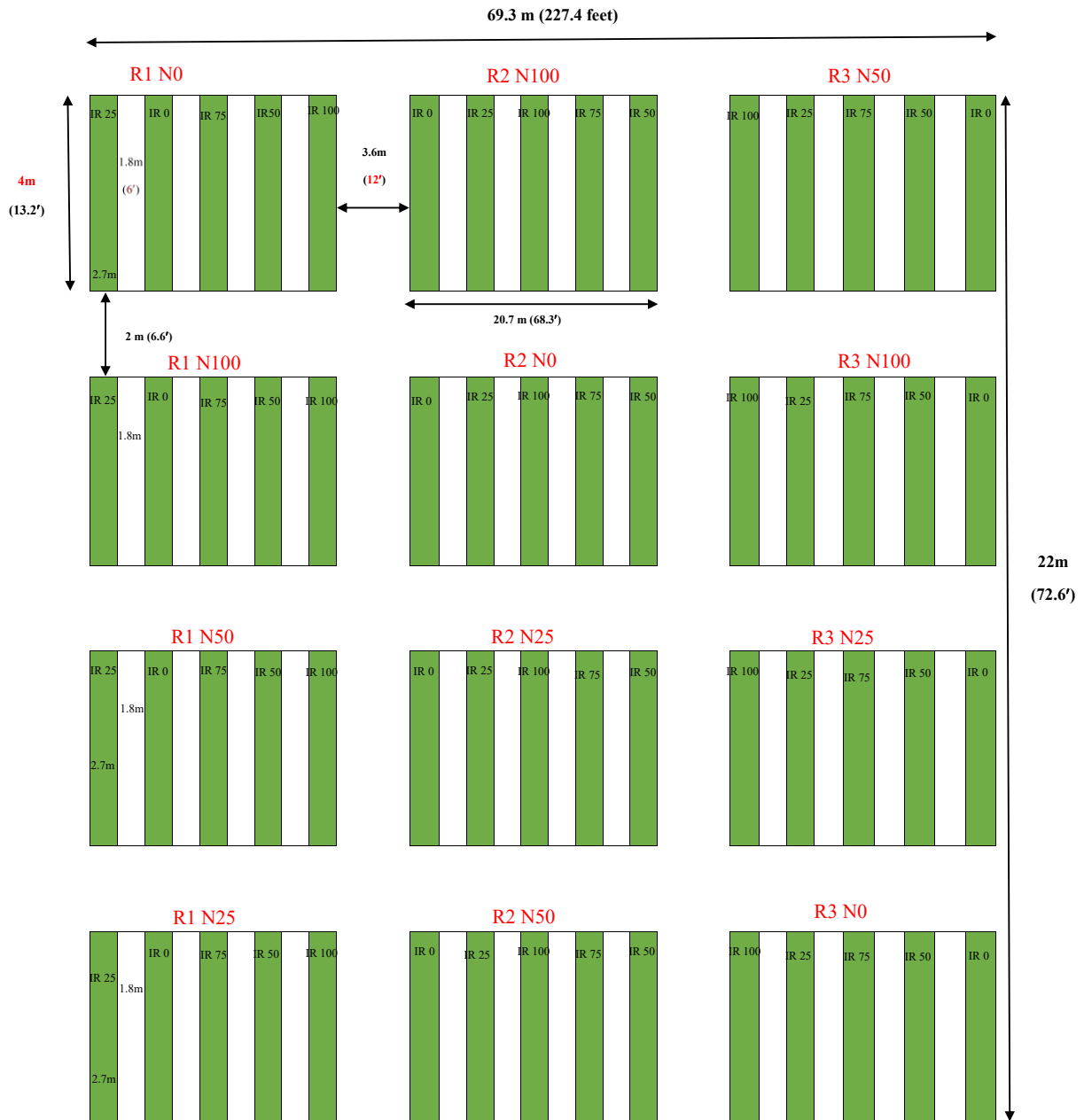
population, it is important to investigate methods to reduce the use of water and chemicals for water conservation, reduction in the production cost, and reduction in environmental impact. UAV-based remote sensing techniques can help significantly reduce the amount of water and nitrogen applications for crop production. The main advantage of UAV-based remote sensing technique is the immediate availability of high-resolution data that can be used to determine the crop performances and stresses of a large area in a short amount of time throughout the growth season for precision agriculture, which aims to optimize the amount of water, fertilizers, and pesticides using site-specific management of crops (Bricco et al, 1998). However, to be useful in a meaningful way for precision agriculture, the remote sensing data must provide the crop nitrogen and water stresses very accurately. This paper presents some of the methods to increase the accuracy of remote sensing data. Ground control points and high-performance GNSS/INS were used to increase the accuracy of remote sensing data. Vegetation indices obtained using remote sensing data were compared with proximal sensor data (Bhandari et al., 2018; Govender et al., 2009) and plant agronomic measurements. Results are shown for strawberry plants.

Experimental Design

Figure 1 shows the experimental strawberry plot design. The test plot has total of three replicate rows (*R1*, *R2*, *R3*), with a 3.6 meter gap between them. The design is a strip-plot design with four nitrogen treatments forming the main plots and four irrigation treatments forming subplots. There are three replications and a total of 60 subplots.

Each row is 22 meters (72.6 feet) long, and is divided into four 4 m x 20.7m (13.2 x 68.3 ft) subplots, with a gap of 2 m (6.6 feet) between the subplots. The large gap between the rows and plots is to avoid the error in data due to nitrogen leaching and water seepage. Each subplot is further divided into five 4 m x 2.7 m subplots with a gap of 1.8 meters between the subplots. The plots are treated with different levels of irrigation, while keeping the level of nitrogen application the same. For example, the first plot (upper left plot in Figure 1) is treated with 0% nitrogen (N0), while each subplot was treated with a different level of irrigation, i.e., 0% irrigation (IR0), 25% (IR25), 50% (IR50), 75% (IR75), and 100% irrigation (IR100). The soil nitrogen level was determined prior to beginning the study by sending the samples of the soil to a soil testing lab. The plots were drip irrigated at 0%, 25%, 50%, 75%, and 100% of irrigation level that is estimated by the evapotranspiration calculations (Bhandari et al, 2018). Similarly, the nitrogen treatment was slow release nitrogen at 0%, 25%, 50%, and 100% of the nitrogen recommended for strawberry growth after taking into account the existing nitrogen in the soil.

The actual water requirement for the strawberry production was determined using the crop evapotranspiration (ET_c), estimated from the potential evapotranspiration (ET_o) (Bhandari et al., 2018; Allen et al., 1998).

Proceedings of the 15th International Conference on Precision Agriculture
June 26-29, 2022, Minneapolis, Minnesota, United States

2

Fig 1. Strawberry plot design.

Figure 2 shows the strawberry being grown using the above design. Markers were placed to distinguish the regions of different irrigation and nitrogen application levels.

Fig 2. Experimental strawberry plot.

**Proceedings of the 15th International Conference on Precision Agriculture
June 26-29, 2022, Minneapolis, Minnesota, United States**

3

UAV and Airborne Sensors

Two different UAV platforms, Matrice 210 and Matrice 600 from DJI, shown in Figure 3, were used for this study.

Fig 3. DJI Matrice 210 (left) and DJI Matrice 600 UAV (right).

The UAVs are equipped with an inertial measurement unit (IMU), GPS receiver, barometer and magnetometer, and autopilots for autonomous flights.

The Matrice 210 UAV is equipped with an Altum multispectral sensor from MicaSense, shown in Figure 3. It is a 5-band multispectral sensor, and captures 5-band spectral data on different wavelengths (blue to NIR). The Matrice 600 is equipped with a Nano Hyperspec sensor from Headwall, also shown in Figure 4. It is a hyperspectral sensor and captures data in 400-1000 nm spectral range, and has 640 spatial bands, 270 spectral bands, and frame rate of 300 Hz. It is also equipped with a high-performance GNSS/INS. GNSS/INS data is used for orthorectification.

Fig 4. RedEdge multispectral sensor (left) and Nano Hyperspec sensor (right).

Proximal Sensors

The proximal sensors used for ground-truthing are a handheld spectroradiometer and chlorophyll content meter, which are shown in Figure 5. Besides using the proximal sensors, agronomic measurements such as plant height and leaf numbers for each treatment level were also measured.

Proceedings of the 15th International Conference on Precision Agriculture
June 26-29, 2022, Minneapolis, Minnesota, United States

4

Fig. 5. Handheld 2 Spectro-radiometer (left), CM 1000 chlorophyll meter right.

Ground Control Points

The ground control points (GCPs) give an important baseline data for remote sensing data correction (Hummel, 2016). A GCP is a physically marked location with a fixed position, and has GPS coordinates that are corresponding to the location of the GCP. GCPs help increase the spatial accuracy of remote sensing data. With the use of well-placed GCPs, the accuracy of remote sensing data can be highly increased and to the level of the accuracy of GPS. While GCPs can help increase the accuracy of remote sensing data, several factors affect how much increase in accuracy can be obtained. Number of GCPs, their distribution and location with respect to the crop field, and the quality of GCPs themselves affect the correction to the remote sensing data they can provide (Guang et al., 2016; Oniga et al., 2018).

Figure 6 shows a GPS equipped GCP, Aeropoints™, from Propeller Aero. Six GCPs were laid in the field. The GCPs give an important baseline data for remote sensing data correction. The GCPs are equipped with GPS to provide the coordinates that are corresponding to the location of the GCP.

Fig 6. Aeropoint™ GCPs from Propeller Aero.

Proceedings of the 15th International Conference on Precision Agriculture
June 26-29, 2022, Minneapolis, Minnesota, United States

5

Data Collection

The airborne and proximal sensor data were collected on a weekly basis. The remote sensing data from the UAVs were collected at close to noon time. Handheld spectroradiometer and chlorophyll data were collected and either before or after the data collection from the UAVs were completed. Figure 7 shows the multispectral data being collected from Matrice 210 UAV.

Fig 7. Strawberry data collection from UAV.

The UAV data were collected from the entire plot each week the data were collected. However, for the proximal sensor data, only a sample of plants were chosen. The spectroradiometer data were collected either at the canopy level or the leaf level using the contact probe with the leaf clip. In addition, plant height and leaf numbers were also measured. Figure 8 shows the plant height for different irrigation levels from the data collected over a period of about 4 weeks. It can be seen that the plant heights show an expected trend with the plant heights being maximum for 100% irrigation level. It can also be noticed that the plant heights are similar for 25% and 50% irrigation levels.
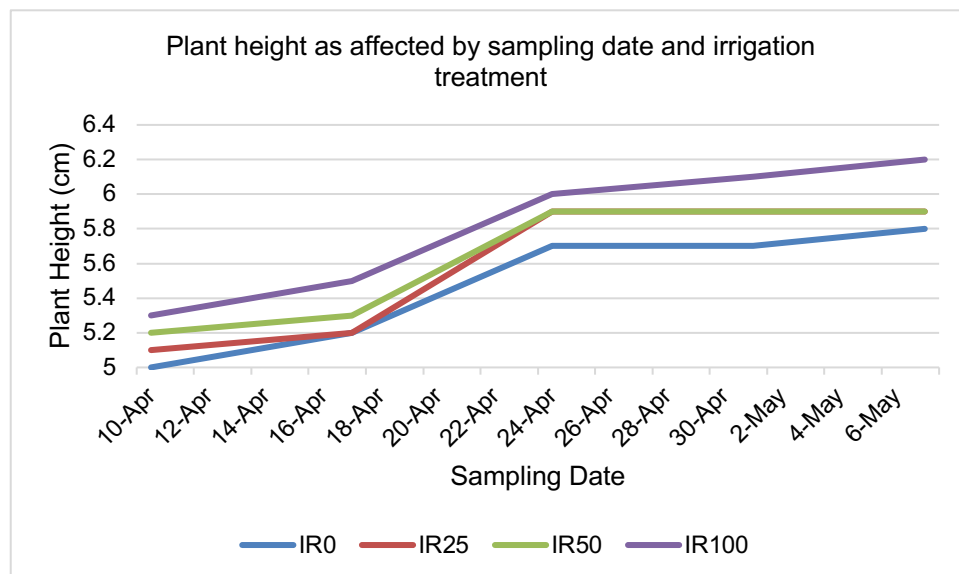

Fig 8. Effect of irrigation level on strawberry plant height.

Figure 9 shows the plant height for different nitrogen treatment levels. A similar trend is seen with the plant height being maximum for 100% nitrogen level and lowest for the 0% nitrogen treatment.
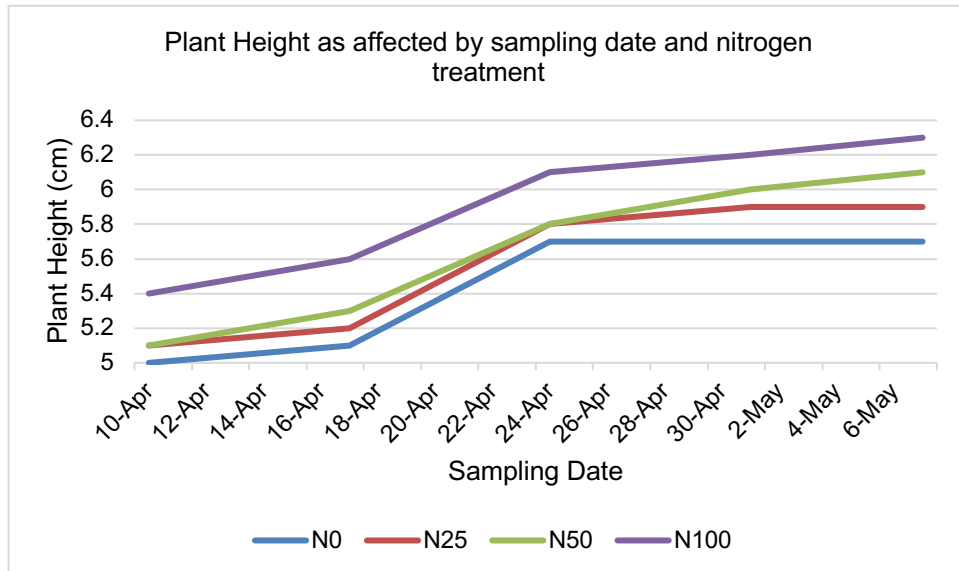
Proceedings of the 15th International Conference on Precision Agriculture
June 26-29, 2022, Minneapolis, Minnesota, United States

6

Fig 9. Effect of nitrogen treatment level on strawberry plant height.

Leaf numbers show similar trends with water and nitrogen treatment levels as shown in Figures 10 and 11. Thus, the strawberry plants in the plot provide a variation in plant health to assess the effectiveness of remote sensing data.
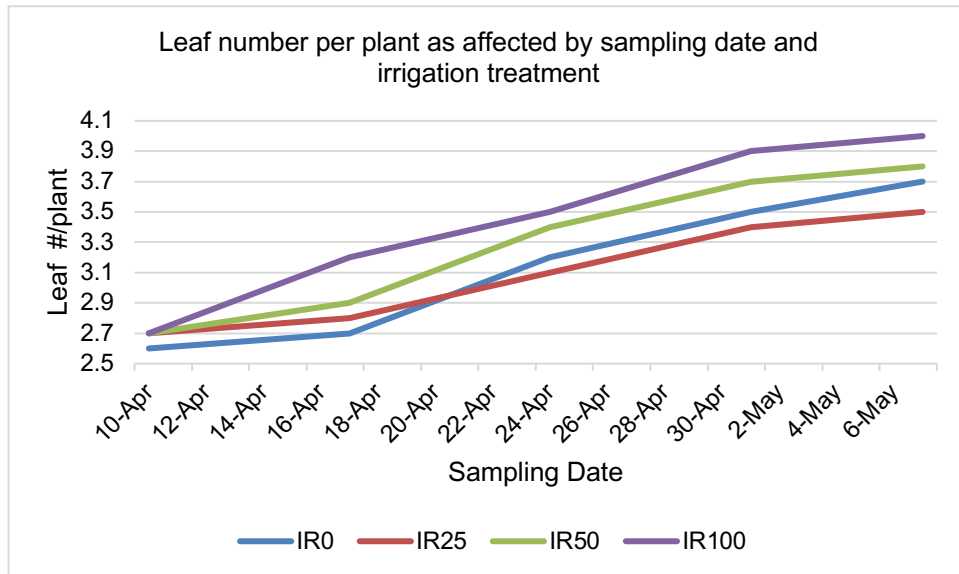

Fig 10. Effect of irrigation level on strawberry plant leaf numbers.

Proceedings of the 15th International Conference on Precision Agriculture
June 26-29, 2022, Minneapolis, Minnesota, United States
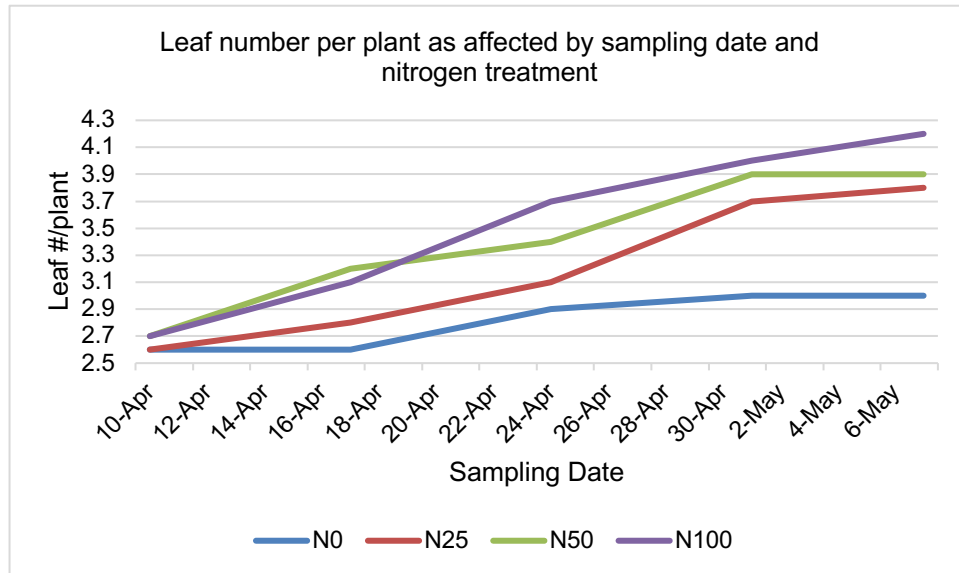
7

Fig 11. Effect of nitrogen treatment level on strawberry plant leaf numbers.

Remote Sensing Data Processing

The multispectral data from UAV was processed using the PrecisionAnalytics software from PrecisionHawk. The collected images are orthomosaicKed by the software, i.e., the individual raw images are orthorectified and then mosaicked to produce a single image. Figure 12 shows the raw image of the strawberry plot. Shown in Figure 13 is the an NDVI image of the strawberry plot.

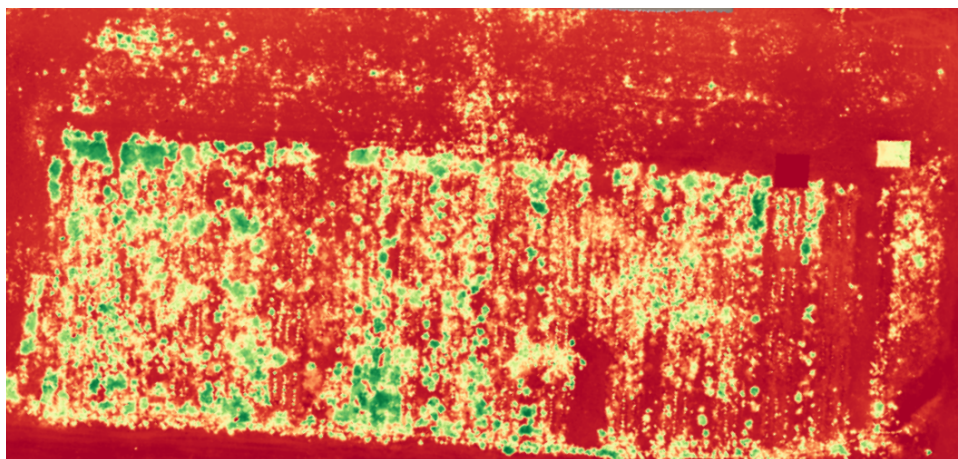**Fig 12. Raw image of the Altum sensor data of the strawberry plot.**

Fig 13. NDVI image of the strawberry plot.

Proceedings of the 15th International Conference on Precision Agriculture
June 26-29, 2022, Minneapolis, Minnesota, United States

8

The AeroPoints ground control data were uploaded wirelessly to the *Propeller* software. The GCPs are solar powered, and after the data collection is completed, the position data are uploaded by pushing a button. Aeropoints data were then imported to the *PrecisionAnalytics* software for processing.

The hyperspectral data collected from the Nano Hyperspec sensor was processed using the Hyperspec III and SpectralView Software from Headwall. The data from each wave-length band is assembled into a three-dimensional hyperspectral 'data cube' (Hyper Cube) for processing and analysis. The hyperspectral cubes, GNSS/INS data, and GNSS correction data was used for postprocessing using POSPac UAV software from Applanix.

Results and Discussion

Using the processed data, several vegetation indices were calculated including normalized difference vegetation index (NDVI), Green NDVI (GNDVI), modified chlorophyll absorption ratio index (MCARI), and leaf chlorophyll index (LCI), water band index (WBI) (Bhandari et al., 2019). For example, the NDVI values are calculated using the following formula:

$$\text{NDVI} = \frac{\rho_{NIR} - \rho_{RED}}{\rho_{NIR} + \rho_{RED}} \quad (1)$$

where ρ_{NIR} and ρ_{RED} are reflectances in the NIR and Red spectrums. NDVI ratio ranges from -1 to 1. Higher positive NDVI values indicate healthy plants whereas lower values indicate unhealthy plants and negative values indicate no vegetation. Specifically, NDVI is used to detect nitrogen stresses.

Similarly, Water Band Index is calculated using the reflectances at 970 nm and 900 nm as given below:

$$\text{WBI} = \frac{\rho_{970}}{\rho_{700}} \quad (2)$$

The higher the water content in vegetation canopies, the stronger the absorption at 970 nm relative to the absorption at 900 nm. These vegetation indices were compared with chlorophyll meter data and vegetation indices calculated using the spectroradiometer.

Figure 14 shows the relationship between the NDVI obtained using the multispectral data and hyperspectral data collected from the UAVs compared with chlorophyll meter data. Multispectral NDVI has a Pearson correlation coefficient (ρ) of 0.80 with CM 1000 data ($\rho = 0.8$), significant at probability level (p) of 4×10^{-6}. NDVI has been used to assess the level of leaf chlorophyll concentration and nitrogen contents.
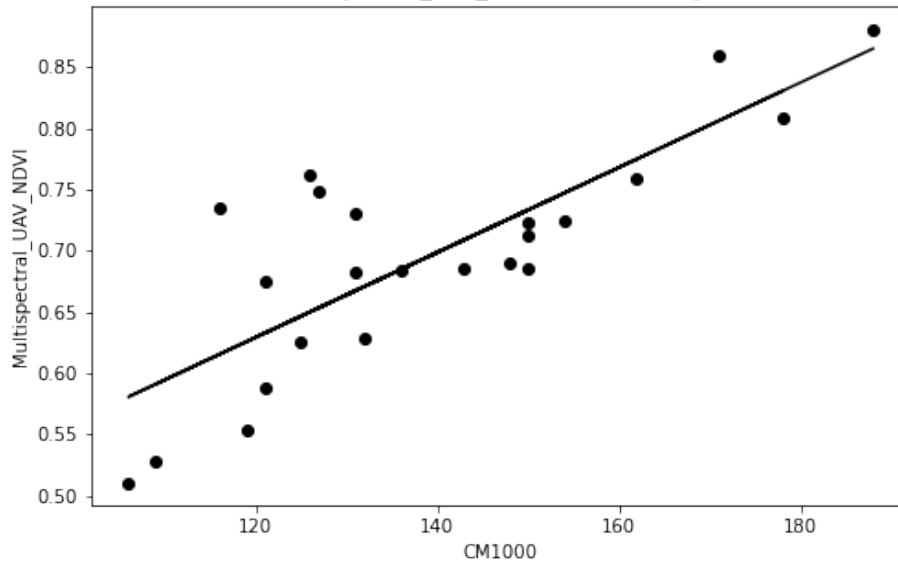
Proceedings of the 15th International Conference on Precision Agriculture
June 26-29, 2022, Minneapolis, Minnesota, United States

9

Fig 14. Relationship between multispectral NDVI and chlorophyll meter data (ρ = 0.8, p = 4 $\times$ 10^{-6}).

The hyperspectral NDVI had slightly lower correlation with the chlorophyll meter data as shown in Figure 15.
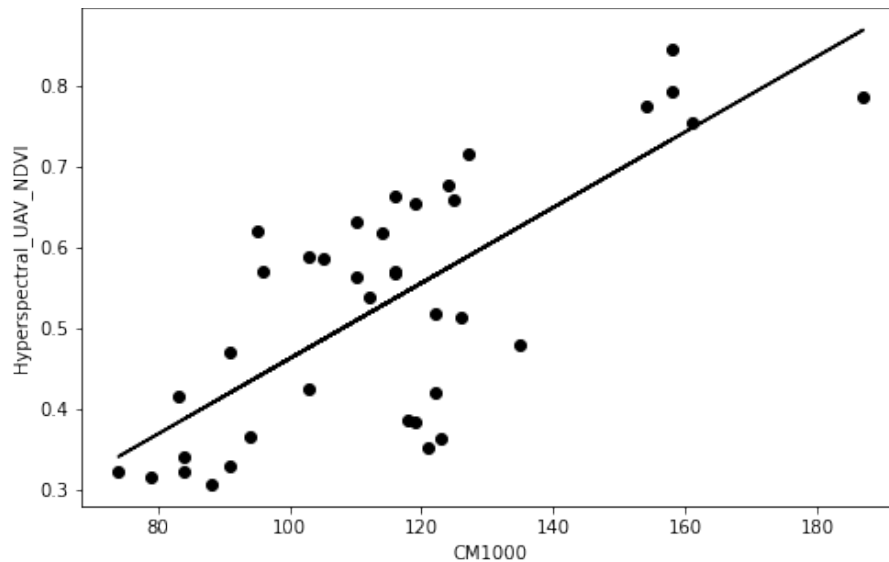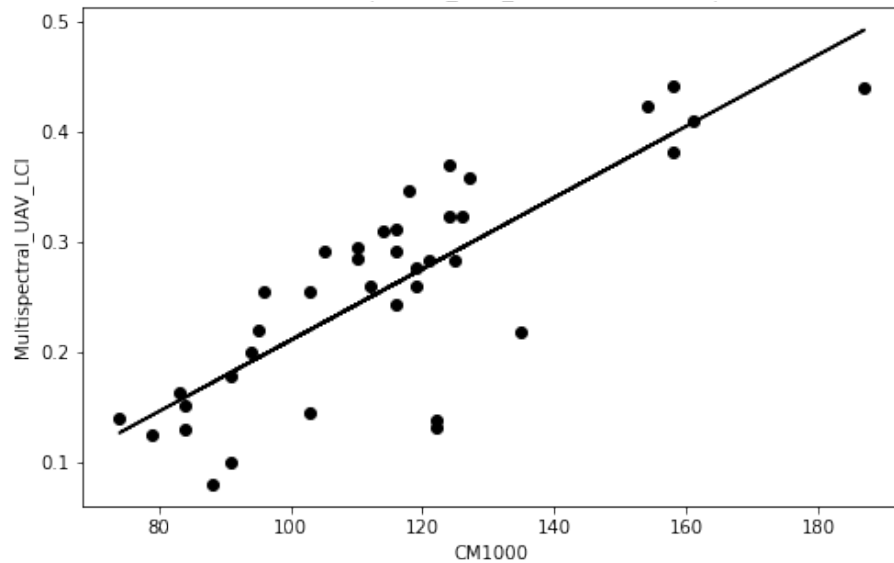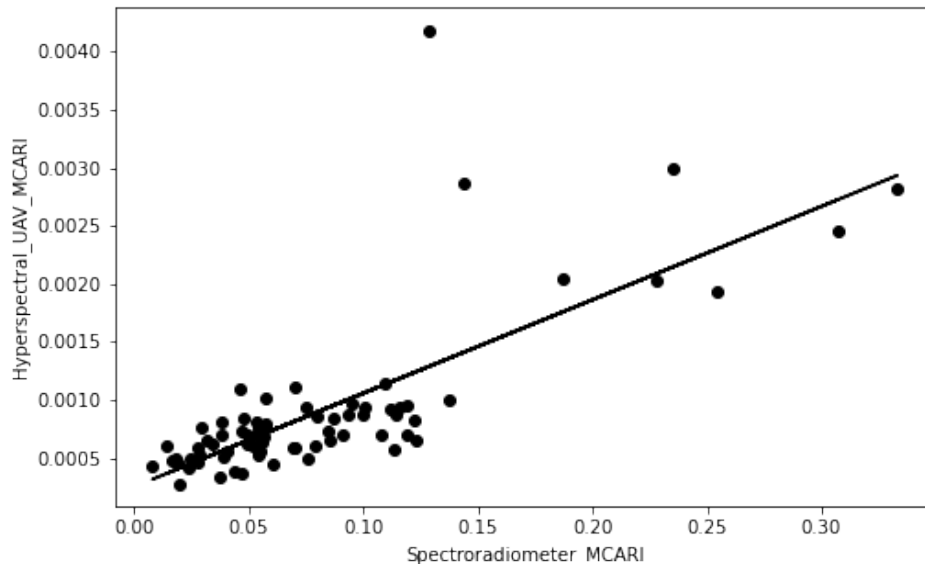

Fig 15. Relationship between hyperspectral NDVI and chlorophyll meter data (ρ = 0.74, p = 10^{-7}).

Figure 16 shows the relationship between the leaf chlorophyll index calculated using Altum sensor compared with the chlorophyll meter data. A correlation of 0.82 was obtained.

Proceedings of the 15th International Conference on Precision Agriculture
June 26-29, 2022, Minneapolis, Minnesota, United States

10

Fig 16. Relationship between multispectral LCI and chlorophyll meter data (ρ = 0.82, $p \cong 0$).

Figures 17 shows the relationship between modified chlorophyll absorption ratio index (MCARI) calculated using hyperspectral data with that calculated using the spectroradiometer data.

Fig 17. Relationship between hyperspectral MCARI and spectroradiometer MCARI (ρ = 0.75, $p \cong 0$).

With the use of GCPs and high performance GNSS/INS, the correlation between the UAV-based remote sensing data and proximal sensor data are significantly improved, and consistently are above 0.75 in most cases. However, WBI calculated using the hyperspectral data showed lower correlation with that calculated using the spectroradiometer data as shown in Figure 18.
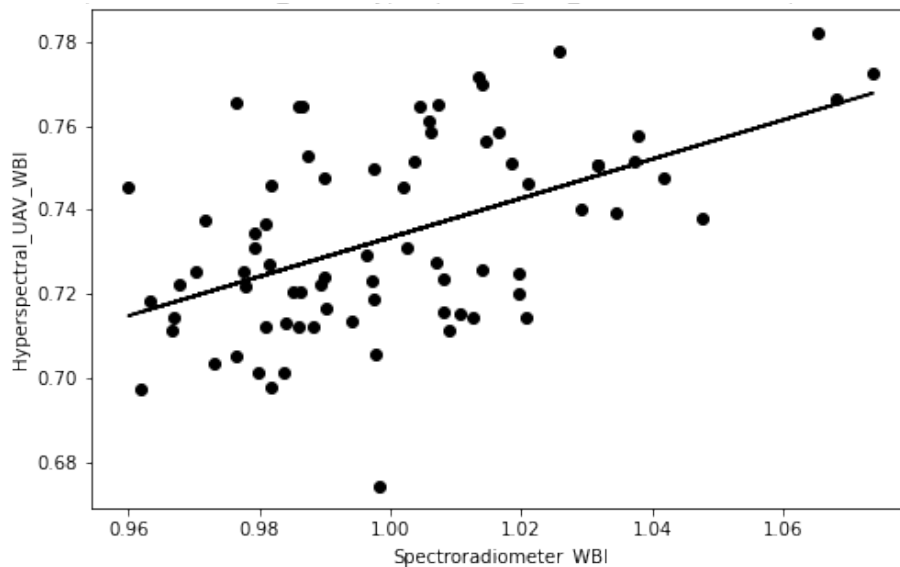
Proceedings of the 15th International Conference on Precision Agriculture
June 26-29, 2022, Minneapolis, Minnesota, United States

11

Fig 18. Relationship between hyperspectral WBI and spectroradiometer WBI (ρ = 0.52, p = 2.3 × 10^{-6}).

Conclusion

This paper showed the effect of portable ground control points and/or high-performance GNSS/INS on the accuracy of remote sensing data. Both the multispectral and hyperspectral data of strawberry plants were collected from UAVs. Also collected were chlorophyll meter and spectroradiometer data along with plant heights and leaf numbers per plant. The experimental design provided a variation in plant water and nitrogen stresses to evaluate the effectiveness of remote sensing data in detecting the plant stresses. The UAV data and spectroradiometer data were used in the calculation of several vegetation indices. The vegetation indices were compared with chlorophyll meter data. Use of GCPs and high-performance GNSS/INSS significantly improved the resolution of the UAV-based remote sensing data. The UAV vegetation indices calculated using the UAV data generally had high degree of correlation with the proximal sensor data. However, the WBI calculated using the hyperspectral UAV data had lower correlation with that calculated using the spectroradiometer data.

Acknowledgements

References

Allen, R. G., Pereira, L. S., Raes, D., & Smith, M. (1998). Crop evapotranspiration: guidelines for computing crop water requirements. In Irrigation and Drainage (Paper No. 56). Food and Agriculture Organization of the United Nations, Rome, Italy.

Bhandari, S., Raheja, A., Chaichi, M., Green, R, Do, D., Ansari, M., et al. (2018). Ground-truthing of UAV-based remote sensing data of citrus plants. SPIE Defense + Commercial Sensing, Proceedings of Autonomous Air and Ground Sensing Systems for Agricultural Optimization and Phenotyping III, Kissimmee, FL.

Bhandari, S., Raheja, A., Chaichi, M., Pham, F., Sherman, T., et al. (2019). Comparing the effectiveness of hyperspectral and multispectral data in detecting citrus nitrogen and water stresses. SPIE Defense + Commercial Sensing, Proceedings of Autonomous Air and Ground Sensing Systems for Agricultural Optimization and Phenotyping IV, Baltimore, MD.

Bricco, B., Brown, R. J., et al. (1998). Precision agriculture and the role of remote sensing: a review. *Canadian Journal of Remote Sensing*, 24(3), 315-327.

Proceedings of the 15th International Conference on Precision Agriculture
June 26-29, 2022, Minneapolis, Minnesota, United States

12

Govendor, M., Dye, P. J., et al. (2009). Review of commonly used remote sensing and ground-based technologies to measure plant water stress. *Water SA*, 35(5), 741-752.

Guang, Y. and Weili, J. (2011). Research on impact of ground control point distribution on image geometric rectification based on Voronoi diagram. *Procedia Environmental Sciences*, 11(A), 365-371.

Habib, A., Han, Y., et al. (2016). Automated ortho-rectification of UAV-based hyperspectral data over an agricultural rield using frame RGB imagery. *Remote Sensing*, 8(10), 796.

Hummel, P. (2016). Remotely sensed ground control points. XXXIII International Society of Photogrammetry, Remote Sensing and Spatial Information Sciences, Prague, Czech Republic.

Oniga, V.-E., Breaban., A.-I., and Statescu, F. (2018). Determining the optimum number of ground control points for obtaining high precision results based on UAS images. 2nd International Electronic Conference on Remote Sensing, 2(7), 352.

Proceedings of the 15th International Conference on Precision Agriculture
June 26-29, 2022, Minneapolis, Minnesota, United States

13